

Cyclometalated Ir(III) Complexes as Lysosome-Targeted Photodynamic Anticancer Agents

Jiayi Zhu,[#] Yan Liu,[#] Zhao Zhang, Xili Yang,^{*} and Feng Qiu^{*}Cite This: *ACS Omega* 2023, 8, 34557–34563

Read Online

ACCESS |



Metrics & More

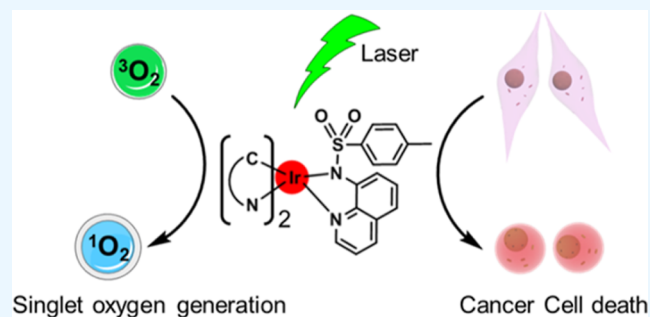


Article Recommendations



Supporting Information

ABSTRACT: We have designed and synthesized two Ir(III) complexes (**Ir1** and **Ir2**) coordinated with an 8-sulfonamidoquinoline derivative ligand as photosensitizers, which exhibit strong red phosphorescence emission and a long phosphorescence lifetime. The Ir(III) complexes exhibit a high population of triplet states, which enable red phosphorescence and efficient singlet oxygen generation. **Ir1** and **Ir2** rapidly enter the cancer cells and accumulate in lysosomes, producing large amounts of intracellular singlet oxygen when exposed to light irradiation, eventually leading to cancer cell death, and the phototoxic indexes of complexes **Ir1** and **Ir2** against cancer cells are in the range of 76–228. Overall, our studies indicate that the synthesized Ir(III) complexes with quinoline ligands exhibit photosensitizing properties, effectively inducing cancer cell death when exposed to light. These promising results suggest their potential application in photodynamic therapy.



INTRODUCTION

Cancer is a major human health threat that urgently needs to be overcome.¹ Noninvasive treatment strategies activated by external stimuli have attracted promising attention for their controllable treatment methods, minimal damage to normal tissues, and significant therapeutic effects.^{2,3} Light has long been used as an external stimulus in many therapeutic processes.^{4,5} As a clinical noninvasive therapeutic method, photodynamic therapy (PDT) has attracted widespread attention and achieved good therapeutic effects.^{6,7} PDT is a technique in which photosensitizers are activated by the light of an appropriate wavelength in the presence of oxygen, producing reactive oxygen species (ROS) by transferring electrons from photosensitizers to oxygen and resulting in oxidative cellular damage and destruction.^{8,9} Various organic and inorganic materials, including organic dyes, semiconductor materials, and metal complexes, can be used as photosensitizers to produce ROS under light stimulation.^{7,10} In particular, metal complexes exhibit rich triplet excited-state properties based on the heavy atom effect, revealing the promising potential for PDT.^{8,11}

Cyclometalated Ir(III) complexes exhibit high fluorescence quantum efficiency and triplet excited-state lifetimes,^{12,13} which facilitate electron transfer with oxygen, resulting in a high singlet oxygen (¹O₂) generation quantum yield.^{14,15} In the past few years, several Ir(III) complexes functioning as photosensitizers for PDT treatment have been reported.^{16–18} In particular, the red-emitting cyclometalated Ir(III) complexes are widely used in PDT.^{19–22} Furthermore, cyclometalated Ir(III) complexes containing different carbon–nitrogen (CN) and diamine (NN) ligands exhibited different phototoxicity indexes (PI, the ratio of

the toxic effects in dark and upon light irradiation) for cancer cells, indicating the key role of ligands in the PDT of cyclometalated Ir(III) complex.^{23–25}

Quinoline derivatives exhibit low cytotoxicity, high cell permeability, and relatively convenient synthetic and functionalization methods and can be used as a versatile ligand for preparation of metal complexes.^{26,27} 8-Quinolinol is a potential radioprotective agent, as a ligand and fluorophore in the Zn(II) complex, which can reduce the acute side effects of radiotherapy in cancer treatment. The synthesis and photophysical properties of quinolinolate-Ir(III) complexes have been reported, but their phosphorescence properties are weak.²⁸ The effect of the quinoline ligand on the singlet oxygen production capacity and PDT efficacy is still unknown.

Based on the above background, we choose 4-methyl-N-quinoline-8-ylbenzenesulfonamide ligand as an ancillary ligand to synthesize two phosphorescent cyclometalated Ir(III) complexes (Figure 1, **Ir1** and **Ir2**) as photosensitizers. We use two different N ligands (N = 1-phenylisoquinoline (1pq) and 2-(2-pyridyl)-benzothiothiophene (pbt)) to modulate the luminescence properties of two cyclometalated Ir(III) complexes. **Ir1** and **Ir2** feature high triplet state population enabling red

Received: May 15, 2023

Accepted: August 28, 2023

Published: September 11, 2023



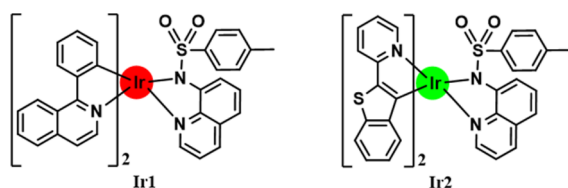


Figure 1. Chemical structures of the cyclometalated Ir(III) complexes (**Ir1** and **Ir2**).

phosphorescence, long phosphorescence lifetime, and efficient singlet oxygen generation. **Ir1** and **Ir2** can rapidly enter the cancer cells and accumulate in lysosomes, producing large amounts of singlet oxygen intracellularly when exposed to the light irradiation and eventually leading to cancer cell death. In these assays, quinoline-functionalized cyclometalated Ir(III) complexes with a high phototoxic potential against cancer cells were identified, suggesting that quinoline functionalization was favorable for the application of cyclometalated Ir(III) complexes in PDT.

RESULTS AND DISCUSSION

Synthesis and Characterization. Two novel cyclometalated Ir(III) complexes (**Ir1** and **Ir2**) containing 4-methyl-*N*-quinoline-8-ylbenzenesulfonamide ligand as the ancillary ligand were synthesized according to the methods in the [Experimental Section](#) (Figure S1). Briefly, the iridium dimer ($[(L)_2Ir(m-Cl)]_2$), ($L = 1pq$ or pbt) was reacted with the 4-methyl-*N*-quinoline-8-ylbenzenesulfonamide ligand in dichloromethane and ethanol ($v/v = 4:1$) overnight. **Ir1** and **Ir2** were purified by Al_2O_3 column chromatography and obtained in relatively high yield, characterized by NMR and electron spray ionization mass spectrometry (ESI-MS) (Figures S2–S9).²⁹

Photophysical Properties. The photophysical properties of the two cyclometalated Ir(III) complexes in different solvents and the effects of the solvent polarity and viscosity on their properties were investigated. The UV–visible absorption and emission spectra of **Ir1** and **Ir2** were measured in different solvents at 25 °C; all of the photophysical data of **Ir1** and **Ir2** are tabulated in [Table 1](#). The complexes showed similar absorption bands (Figure 2); both complexes displayed strong absorption at 250–300 nm, which was attributed to spin-allowed ligand center transition (1LC), and a weaker absorption at 400–500 nm due to a combination of spin-allowed metal-to-ligand charge transfer (1MLCT) and ligand-to-ligand charge transfer (1LLCT) characters. **Ir1** and **Ir2** showed a weak absorption between 400 and 500 nm assigned to the spin-forbidden of 3MLCT and 3LLCT transitions, which were compared with similar reported ionic iridium(III) complexes.^{30,31} **Ir1** and **Ir2** exhibited strong red phosphorescence between 580 and 630 nm, and their emission quantum yields are comparable to the standard $Ru(bpy)_3Cl_2$ (Figure 2b, [Table 1](#)), at room temperature upon excitation at 455 nm. Notably, **Ir1** and **Ir2** exhibited polarity-sensitive UV–vis absorption and phosphorescence,

higher UV–vis absorption, and fluorescence intensity in low-polarity solvents, such as dichloromethane solution.³²

Since the complexes exhibited higher UV–vis absorption and fluorescence intensity in nonpolar solvents, we investigated their phosphorescence intensity in different polarities of solvents composed of water-1,4-dioxane. As shown in [Figure S10](#), as the proportion of 1,4-dioxane increases, the phosphorescence intensity of the complexes was greatly enhanced. Furthermore, oxygen severely affected the phosphorescence intensity ([Figure S11](#)) and lifetime ([Figure S12](#)) of **Ir1** and **Ir2**, which was longer in methylene chloride than in ultrapure water.

Aqueous Stability. A good photosensitizer should have high stability for the anticancer application.³³ Therefore, we monitored the stability of **Ir1** and **Ir2** by UV–vis absorption spectroscopy. As shown in [Figure S13](#), no obvious changes in the absorption spectra of **Ir1** and **Ir2** can be observed in phosphate-buffered saline (PBS) at 25 °C for 24 h. Additionally, **Ir1** and **Ir2** also showed high photostability under 465 nm light (6.5 mW/cm²) irradiation for 1 h and were also stable at different pH values ([Figure S14](#)) and temperatures ([Figure S15](#)).

Cellular Localization. Since **Ir1** and **Ir2** showed excellent phosphorescence in extracellular experiments, **Ir1** and **Ir2** were selected to be used in subsequent experiments for intracellular experiments. The intracellular localization of **Ir1** and **Ir2** was monitored by a confocal microscope. After Hep-G2 cells adhered to the confocal dish, the complexes were incubated with Hep-G2 cells for 1 h. Both complexes emitted red phosphorescence in the cytoplasm of the Hep-G2 cells. In order to study their subcellular localization more accurately, we used commercial organelles dyes (Mito-Tracker Red, ER-Tracker Red, and Lyso-Tracker Red) for coinubation with Hep-G2 cells for 0.5 h to stain the mitochondria, endoplasmic reticulum, and lysosomes. As shown in [Figures 3](#) and [4](#), the bright phosphorescence points of these complexes mainly have high overlap coefficients with the organelles of lysosomes, which shows that the complexes have high targeting efficiency and can be used for lysosome-targeted photosensitizers.

Cytotoxicity Test. Through 3-(4,5-dimethylthiazol-2-yl)-2,5-diphenyltetrazolium bromide (MTT) toxicity test, the dark- and photocytotoxicity of **Ir1** and **Ir2** was investigated against a variety of cells, including liver cancer cell line (Hep-G2), lung cancer cell line (A549), cisplatin-resistant lung cancer cell line (A549R), cervical cancer cell line (Hela), and normal liver cell line (L02). [Table 2](#) summarizes the toxicity of iridium complexes and cisplatin (used as controls) to various cancer cell lines for 48 h under dark and 465 nm light (6.5 mW/cm²) for 0.5 h. IC_{50} is called the half-inhibition rate, which represents the concentration required to inhibit half the cell proliferation and is negatively related to toxicity. The experimental results show that these complexes have very low cytotoxicity in the dark for all cancer cells and normal cells after 48 h of drug exposure and incubation ([Figure S16](#)). However, for photocytotoxicity screening, the IC_{50} of both iridium complexes with four different types of cancer cells is lower than that of cisplatin, and **Ir1** and

Table 1. Photophysical Data of Complexes at 298 K

complexes	λ_{abs}/nm (H ₂ O)	λ_{em} (max)/nm (H ₂ O)	quantum yield (Φ_{em}) ^a (CH ₃ CN)	quantum yield Φ (1O_2) ^b (H ₂ O)	lifetime (τ)/ns (CH ₃ CN) (Air/N ₂)
Ir1	350, 450	610	0.035	0.65	352.6/568.8
Ir2	340, 460	600	0.028	0.68	353.9/383.2

^a Φ_{em} , the luminescence quantum yields. ^b Φ (1O_2), 1O_2 quantum yield. $[Ru(bpy)_3]^{2+}$ was used as a standard compound ($\Phi_{em} = 0.028$, Φ (1O_2) = 0.2, 465 nm light irradiation).

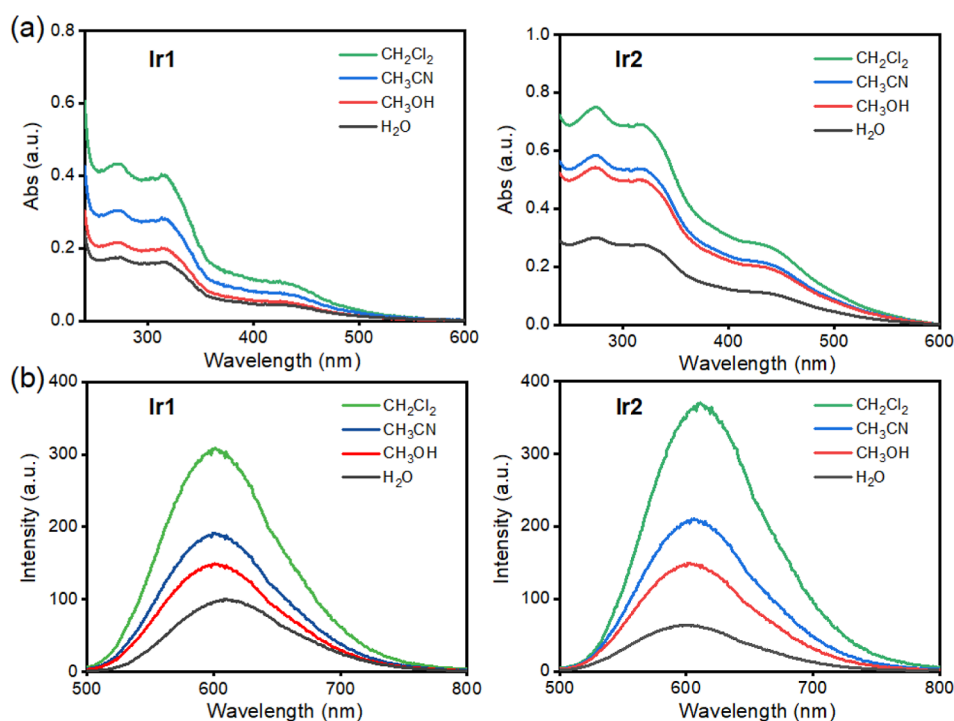


Figure 2. UV-vis (a) and emission spectra (b) of 10 μM Ir1 or Ir2 in various solvents (CH_2Cl_2 , CH_3CN , CH_3OH , and H_2O), $l_{\text{ex}} = 455 \text{ nm}$.

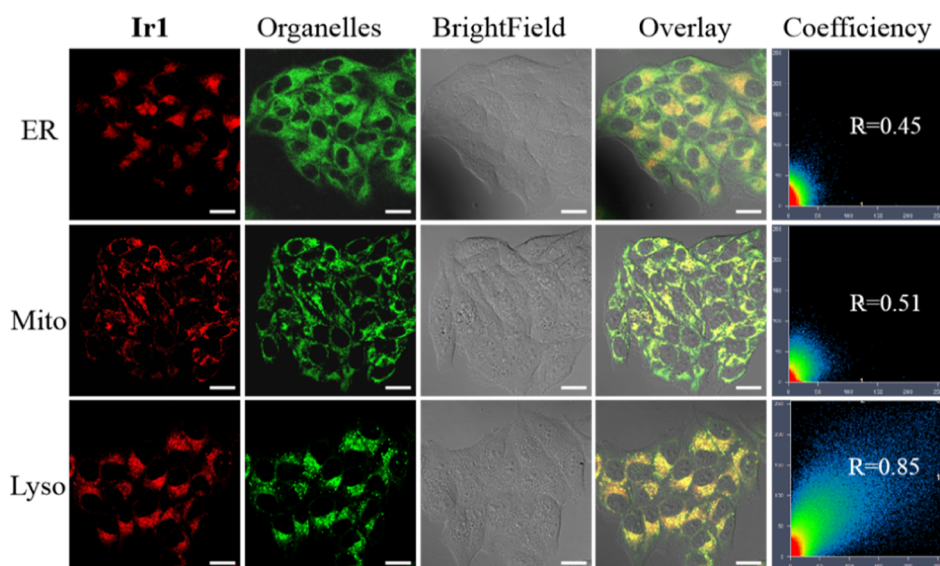


Figure 3. Colocalization images of the Hep-G2 cells costained with Ir1 (10 μM , 1 h, $l_{\text{ex}} = 458 \text{ nm}$, $l_{\text{em}} = 600 \pm 30 \text{ nm}$) and commercial organelles dyes: ER-Tracker Red (333 nM, 30 min, $l_{\text{ex}} = 543 \text{ nm}$, $l_{\text{em}} = 615 \pm 30 \text{ nm}$); Mito-Tracker Red (100 nM, 30 min, $l_{\text{ex}} = 543 \text{ nm}$, $l_{\text{em}} = 599 \pm 30 \text{ nm}$); and Lyso-Tracker Red (75 nM, $l_{\text{ex}} = 543 \text{ nm}$, $l_{\text{em}} = 590 \pm 30 \text{ nm}$). Scale bar: 20 nm.

Ir2 exhibited high photocytotoxicity (IC_{50} less than 5 μM) to HeLa and A549 with a high photocytotoxicity index [PI, ratio of $\text{IC}_{50}(\text{dark})/\text{IC}_{50}(\text{light})$] of more than 110, which indicates that the complexes are highly effective on cancer cells under light. Importantly, Ir1 and Ir2 showed very strong photocytotoxicity against cisplatin-resistant lung cancer cell, A549R, with IC_{50} values of 13.2 and 12.7 ± 0.2 , respectively (Figure 5). While the IC_{50} value of cisplatin was above 50 μM (Figure S17), the above results suggest that cyclometalated Ir(III) complexes have great potential in cancer PDT. In addition, both Ir1 and Ir2 were virtually noncytotoxic to normal liver L02 cells in the absence of light irradiation (the IC_{50} value was above 100 mM, Figure S18).

The excellent photodynamic anticancer properties of the complexes prompted us to investigate their in vivo safety. Zebrafish with vascular expression of green fluorescent protein (GFP) were used to investigate the biosafety of the complexes at the in vivo level. No damage was observed in the vessels of zebrafish treated with Ir1 or Ir2 for 96 h (Figure S19). The above results indicated that Ir1 and Ir2 were promising photosensitizer drugs for efficient PDT.

ROS Generation. The $^1\text{O}_2$ generation quantum yields of the complex were measured by a commonly method. $^1\text{O}_2$ oxidized the imidazole derivative to form a *trans*-annular peroxide adduct, which quenched the absorbance of *p*-nitrosodimethyl aniline

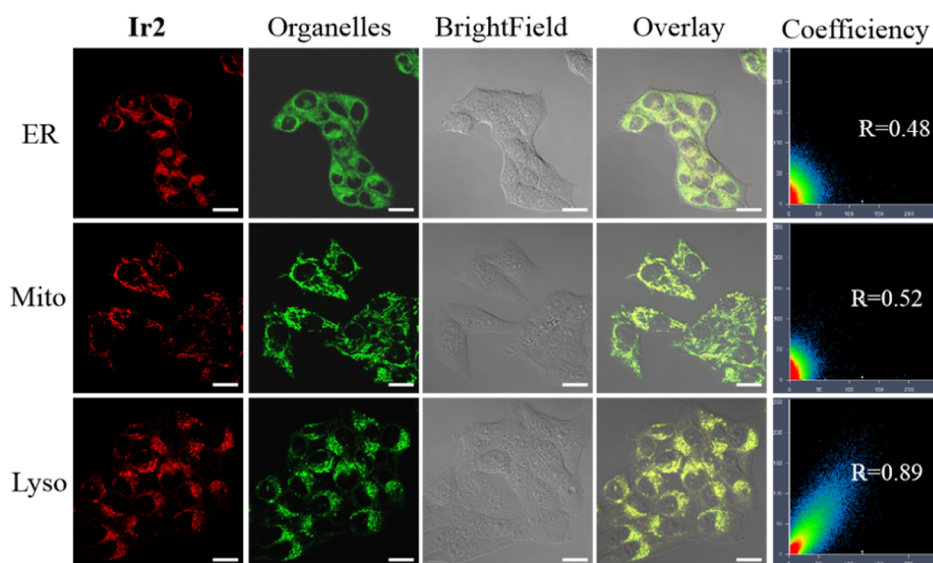


Figure 4. Colocalization images of the Hep-G2 cells costained with Ir2 (10 μ M, 1 h, I_{ex} = 458 nm, I_{em} = 600 \pm 30 nm) and commercial organelles dyes: ER-Tracker Red (333 nM, 30 min, I_{ex} = 543 nm, I_{em} = 615 \pm 30 nm); Mito-Tracker Red (100 nM, 30 min, I_{ex} = 543 nm, I_{em} = 599 \pm 30 nm); and Lyso-Tracker Red (75 nM, 30 min, I_{ex} = 543 nm, I_{em} = 590 \pm 30 nm). Scale bar: 20 μ m.

Table 2. Cytotoxicity (IC₅₀, mM) of the Complexes toward Cancer Cell Lines^a

complex	Hep-G2		Hela		A549		A549R	
	light (dark)	PI ^b	light (dark)	PI ^b	light (dark)	PI ^b	light (dark)	PI ^b
Ir1	4.3 \pm 0.2 (>100)	>23.2	0.5 \pm 0.3 (>100)	>200	0.8 \pm 0.2 (>100)	>133	13.2 \pm 0.2 (>100)	>7.8
Ir2	0.4 \pm 0.2 (>100)	>228	0.7 \pm 0.1 (>100)	>153	0.9 \pm 0.1 (>100)	>113	12.7 \pm 0.2 (>100)	>7.9
Cisplatin	21.8 \pm 0.2 (24.8 \pm 0.2)	1.14			43.2 \pm 2.3 (48.2 \pm 2.7)	1.11	57.5 \pm 1.7 (60.7 \pm 1.7)	1.06

^aData are presented as the means \pm standard deviations. ^bPI = IC₅₀(dark)/IC₅₀(light).

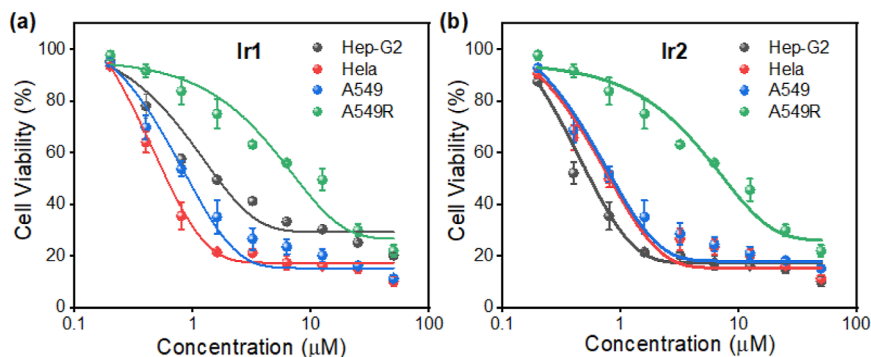


Figure 5. Cytotoxic effects of Ir1 (a) or Ir2 (b) on different types of cells with 465 nm light irradiation.

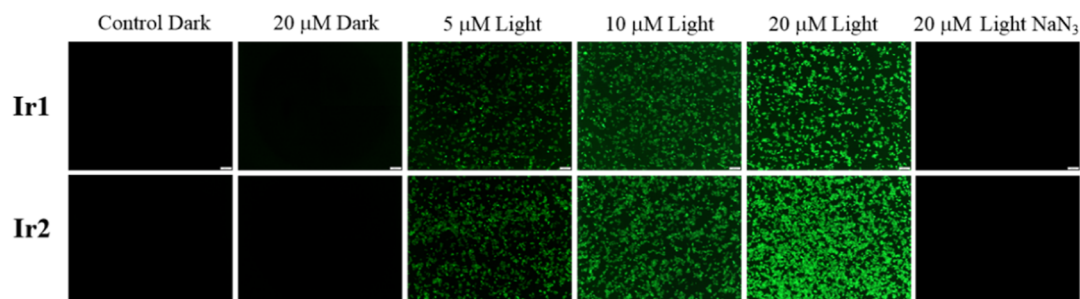


Figure 6. Analysis of ROS generation by Ir1 and Ir2 mediated by PDT using fluorescence microscopy. Hep-G2 cells were incubated with Ir1 or Ir2 for 1 h and irradiated with blue light (465 nm, 6.5 mW/cm²) for 10 min. Scale bar: 200 μ m.

(RNO) to quantify ¹O₂, and the results are presented in Figure S20 and Table 1.³⁴ As can be seen from the picture, the singlet

oxygen yield of the complexes in acetonitrile was higher than that of the standard compound.

Furthermore, as a site of oxidative metabolism in eukaryotes, mitochondria are the main source of ROS, and the PDT process has been reported to cause lysosomal damage by ROS. Confocal microscopy was used to detect the increase of ROS in liver cancer cells induced by **Ir1** or **Ir2**. Hep-G2 cells were incubated with **Ir1** or **Ir2** for 1 h, and then, Hep-G2 was treated with 2',7'-dichlorodihydrofluorescein diacetate (H₂DCFDA) staining for 0.5 h and finally irradiated under 465 nm light (6.5 mW/cm²) for 10 min. Confocal images clearly show that accompanied by the generation of ROS, the green fluorescence intensity of DCF increased in a concentration-dependent manner (Figure 6). Compared with the control cells without light treatment, the fluorescence intensity of DCF increased significantly in cells treated with complexes and irradiation. In addition, the cells pretreated with sodium azide (NaN₃, an effective ¹O₂ scavenger) significantly inhibited the fluorescence signal of the DCF.

CONCLUSIONS

In conclusion, we have reported two red luminescent 8-sulfonamidoquinoline ligand-functionalized cyclometalated Ir(III) complexes that accumulated in the lysosomes of cancer cells. These complexes display high ¹O₂ quantum yields upon 465 nm light irradiation. The phototoxic indexes of complexes **Ir1** and **Ir2** against cancer cells are in the range 76–228. Therefore, it can be used as a highly effective photodynamic therapeutics agent.

EXPERIMENTAL SECTION

Materials and Instruments. IrCl₃·H₂O, 1-phenylisoquinoline(1pq), 2-(2-pyridyl)-benzothioephene (pbt), MTT, DMSO-*d*₆, and PBS were obtained from Macklin. Cervical cancer cell line (Hela), human lung carcinoma cell line(A549), cisplatin-resistant A549 (A549R), human liver cancer cell line (Hep-G2), and human normal liver cell line (L02) were obtained from the ATCC cell bank. Dulbecco's modified Eagle's medium (DMEM) and fetal calf serum were purchased from Sigma-Aldrich. Mito-Tracker Red, ER-Tracker Red, and Lyso-Tracker Red were obtained from Beyotime Biotechnology.

¹H NMR and ¹³C NMR spectra data were obtained utilizing a BrukerAV-500 spectrometer. ESI-MS data were recorded using Agilent 6130B. UV–vis absorption spectra were measured using a UV-2550 spectrophotometer. The fluorescence spectra were recorded with a Hitachi F-7000 Fluorimeter.

Preparation of the Iridium Complex. The specific synthesis steps are as follows: The precursors were prepared from iridium chloride (IrCl₃) and 1-phenylisoquinoline (1 pq) or 2-(2-pyridyl)-benzothioephene (pbt). Specifically, 0.05 mmol of solid iridium chloride and 0.1 mmol of 1 pq or pbt powder were added to 40 mL of solution containing ethylene glycol ether and water (v/v = 3:1) in a two-neck round-bottom flask; the mixture was stirred at 120 °C and refluxed overnight in a nitrogen atmosphere. After the reaction solution was cooled to ambient temperature, it was filtered under vacuum. The precipitate was washed 3 times with diethyl ether.

Next, a mixture of dichloro-bridged dimeric (0.1 mmol) complexes ([L]₂Ir(m-Cl)]₂, (L = 1 pq or pbt), 8-(tosylamino)quinoline (tlq) (0.22 mmol), and triethylamine (4.5 mmol) was completely dissolved in dichloromethane and ethanol (v/v = 4:1) in a sealed reaction container according to the measured molar ratio. The mixture was then refluxed for 20 h in a nitrogen atmosphere and heated at 55 °C. After the solvent

was removed under vacuum filtration, the precipitate was washed with ethanol to remove unreacted ligands and dried under vacuum to obtain solid products **Ir1** or **Ir2**.

[Ir(1pq)₂(tlq)]Cl (Ir1). Yield = 51.6% (92.68 mg). Red color solid. ¹H NMR (500 MHz, DMSO-*d*₆): δ 8.94–8.89 (t, J = 7.5 Hz, 2H), 8.86 (d, J = 6.5 Hz, 1H), 8.29 (d, J = 8.3 Hz, 1H), 8.24 (d, J = 7.9 Hz, 1H), 8.14 (d, J = 8.0 Hz, 1H), 8.06–8.01 (m, 2H), 7.97 (d, J = 8.0 Hz, 1H), 7.84 (dd, J = 6.6, 3.2 Hz, 4H), 7.62 (d, J = 6.6 Hz, 1H), 7.49 (d, J = 7.6 Hz, 2H), 7.47–7.43 (t, J = 7.5 Hz, 1H), 7.38–7.33 (t, J = 8.0 Hz, 2H), 7.28 (d, J = 7.9 Hz, 1H), 7.03 (t, J = 7.0 Hz, 1H), 6.88–6.78 (m, 4H), 6.62 (d, J = 7.3 Hz, 1H), 6.57 (d, J = 8.1 Hz, 2H), 6.21 (d, J = 7.6 Hz, 1H), 6.12 (d, J = 7.8 Hz, 1H), 1.96 (s, 3H) ppm. ESI-MS (*m/z*): Calcd for C₄₆H₃₃N₄O₂S(¹⁹³Ir) (M⁺), 899.07; found, 899.20 [M⁺]. Elemental Anal. Calcd for **Ir1** C₄₆H₃₃N₄O₂SIr: C, 61.39; H, 3.67; N, 6.23; S, 3.56. Found: C, 61.26; H, 3.64; N, 6.32; S, 3.52.

[Ir(pbt)₂(tlq)]Cl (Ir2). Yield = 77.0% (144 mg). Yellow color solid. ¹H NMR (500 MHz, DMSO-*d*₆): δ 9.10 (d, J = 5.7 Hz, 1H), 8.37 (d, J = 8.3 Hz, 1H), 7.94–7.84 (m, 4H), 7.80 (d, J = 7.9 Hz, 1H), 7.71 (d, J = 8.0 Hz, 1H), 7.61 (t, J = 5.8 Hz, 2H), 7.51 (t, J = 8.1 Hz, 1H), 7.42 (dd, J = 8.4, 5.0 Hz, 1H), 7.32 (d, J = 8.0 Hz, 1H), 7.24 (dd, J = 15.4, 6.3 Hz, 2H), 7.17 (t, J = 7.6 Hz, 1H), 7.09 (t, J = 7.5 Hz, 1H), 6.94–6.89 (m, 5H), 6.82 (dt, J = 18.9, 7.7 Hz, 2H), 6.05 (d, J = 8.1 Hz, 1H), 5.97 (d, J = 8.1 Hz, 1H), 2.23 (s, 3H). ESI-MS (*m/z*): Calcd for C₄₂H₂₉N₄O₂S₃(¹⁹³Ir) (M⁺), 910.12; found, 933.00 [M⁺+Na]⁺. Elemental Anal. Calcd For **Ir2** C₄₂H₂₉N₄O₂S₃Ir: C, 55.38; H, 3.19; N, 6.15; S, 10.55. Found: C, 55.36; H, 3.14; N, 6.18; S, 10.52.

HPLC Investigation. The prepared 50 μM **Ir1** or **Ir2** solutions contained 1% DMSO in PBS/acetonitrile (CH₃CN) (V/V, 3:7). Analytical high-performance liquid chromatography (HPLC) was used for analysis with an injection volume of 20 μL. The mobile phase was a linear gradient of 0.1% HCOOH in H₂O and 0.1% HCOOH in CH₃CN. The absorbance wavelength was set to 280 nm. Each sample was analyzed by a high-performance liquid chromatograph (Thermo Fisher) equipped with a C18–H HPLC column at a flow rate of 1.0 mL/min and a column temperature of 25 °C. Retention time for **Ir1** is 3.108 min and that for **Ir2** is 2.867 min.

Cellular Localization. Hep-G2 cells were placed in 35 mm confocal dishes for about 12 h and then incubated with 10 mM **Ir1** or **Ir2** for 1 h before staining with Lyso-Tracker, Mito-Tracker, or ER-Tracker for 30 min. Cells were washed with PBS and imaged with confocal microscopy.

Dark Cytotoxicity and Phototoxicity. Hela, A549, A549R, Hep-G2, and L02 cells were cultured in mixed DMEM supplemented with 10% v/v FBS and 1% v/v penicillin–streptomycin and maintained in a humidified incubator at 37 °C under an atmosphere of 5% CO₂.²⁹

The cytotoxicity of complexes **Ir1**, **Ir2**, and cisplatin on A549, A549R, Hela, and Hep-G2 cells for 48 h was evaluated by a colorimetric MTT assay. First of all, about 5000 of each kind of cells were plated and seeded per well in 96-well plates; then, the cells were incubated with the complexes in different concentrations at 37 °C. In the dark toxicity, the complexes' exposure period was 48 h. As for phototoxic operations, after the cells were incubated with complexes **Ir1** or **Ir2** for 1 h, the complexes were removed, and the 96-well plate was rinsed twice with PBS, and then, the nondrug medium was placed. After that, the 96-well plate was irradiated with 465 nm light for 30 min and then cultured in the incubator for another 47.5 h. Subsequently, MTT (25 μL, 5 mg/mL) was added and incubation continued

for 4 h to form purple formazan. Finally, 100 μL of DMSO was added to each well to dissolve purple formazan, and the absorbance at 490 nm was recorded by a microplate reader. Cells in the blank control group were treated with DMSO (1%, v/v).

Determination of Singlet Oxygen Quantum Yield. An air saturation of acetonitrile solution, containing the complexes under test ($A = 0.1$ at 405 nm), *p*-nitrosodimethyl aniline (RNO, 24 μM), and imidazole (12 mM) in a quartz fluorescent cuvette, was irradiated at 405 nm, and the absorbance was recorded at various time intervals. Plots of $A_0 - A$ at 420 nm (A_0 is the absorbance before irradiation) versus the irradiation time were prepared, and the linear regression slope was calculated (S_{complex}). Phenalenone was used as the reference compound ($\Phi_{\text{ref}}(^1\text{O}_2) = 95\%$) to obtain S_{ref} and then to calculate the singlet oxygen quantum yields (Φ_{complex}) for each complex

$$\Phi_{\text{complex}} = \Phi_{\text{ref}} * S_{\text{complex}} / S_{\text{ref}} * I_{\text{ref}} / I_{\text{complex}} \quad (1)$$

$$I = I_0 * (1 - 10^{-A}) \quad (2)$$

where I (absorbance correction factor) was calculated from eq 2, I_0 is the light intensity of the irradiated source, and A is the absorbance of the complex.

Determination of Intracellular ROS. ROS accumulation in Hep-G2 cells induced by **Ir1** or **Ir2** under light irradiation was evaluated by a fluorescence microscope and 2',7'-dichlorofluorescein diacetate (H_2DCFDA). DCFH-DA is an ROS fluorescent probe that diffuses into the cell and is rapidly oxidized by intracellular ROS to form the highly fluorescent 2',7'-dichlorofluorescein (DCF, $\lambda_{\text{ex}} = 488$ nm, $\lambda_{\text{em}} = 520 \pm 20$ nm). The fluorescence intensity of DCF is believed to be positively correlated with the amount of ROS formed in cells.

Biosafety in Zebrafish. The GFP-transfected Singapore zebrafish (<5 bpf) were obtained from the Center of Experiment Animals at Sun Yat-Sen University. Zebrafish were housed in E3 medium in 12-well plate dishes (five zebrafish per well) at 28 $^\circ\text{C}$.

Zebrafish were incubated with 50 μM **Ir1** or **Ir2** for 96 h. And then, all zebrafish were exposed to E3 medium with anesthetic tricaine (0.2 mg/mL). Zebrafish mortality and the fluorescence of GFP were visualized with an Olympus X151 microscope. GFP: $\lambda_{\text{ex}} = 460 \pm 20$ nm, $\lambda_{\text{em}} = 530 \pm 20$ nm.³⁰

■ ASSOCIATED CONTENT

SI Supporting Information

The Supporting Information is available free of charge at <https://pubs.acs.org/doi/10.1021/acsomega.3c03234>.

Experimental synthetic routes, ^1H NMR spectrum of **Ir1**, ^{13}C NMR spectrum of **Ir1**, ESI-MS spectrum of **Ir1**, ^1H NMR spectrum of **Ir2**, enlarged aromatic region of ^1H NMR spectrum of **Ir2**, ^{13}C NMR spectrum of **Ir2**, ESI-MS spectrum of **Ir2**, HPLC spectra of the **Ir1** and **Ir2**, emission spectra of **Ir1** and **Ir2** in various polar 1,4-dioxane-water systems, emission spectra of **Ir1** and **Ir2** in CH_3CN under N_2 and air atmospheres, phosphorescence lifetimes of **Ir1** and **Ir2**, photostability of **Ir1** and **Ir2**, stability of **Ir1** and **Ir2** in PBS solution with varying pH from 4 to 10, stability of **Ir1** and **Ir2** in PBS solution with different temperatures from 25 to 55 $^\circ\text{C}$, cytotoxic effects of **Ir1** or **Ir2** on different types of cells in the dark condition, cell viabilities of cisplatin on different types of cells with or without light irradiation, cell viabilities of L02 cell incubation with different concentrations of **Ir1** or **Ir2** with or without light irradiation, toxicity of **Ir1** and **Ir2** in

zebrafish for 48 or 96 h, and determination of the $^1\text{O}_2$ quantum yield of **Ir1** and **Ir2** (PDF)

■ AUTHOR INFORMATION

Corresponding Authors

Xili Yang – Department of Cardiology, The First People's Hospital of Foshan, Foshan 528000, China; orcid.org/0000-0001-8105-6644; Email: xiliyang0277@163.com

Feng Qiu – Department of Laboratory Medicine, The Seventh Affiliated Hospital of Southern Medical University, Foshan 516006, China; Email: QFSFL@126.com

Authors

Jiayi Zhu – Department of Cardiology, The First People's Hospital of Foshan, Foshan 528000, China

Yan Liu – Guangdong Provincial Key Laboratory of Sensor Technology and Biomedical Instrument, School of Biomedical Engineering, Shenzhen Campus of Sun Yat-sen University, Sun Yat-Sen University, Shenzhen 518107, China

Zhao Zhang – Department of Biochemistry and Molecular Biology, Guangdong Medical University, Zhanjiang 524023, China; orcid.org/0000-0002-3996-9893

Complete contact information is available at:

<https://pubs.acs.org/10.1021/acsomega.3c03234>

Author Contributions

[#]J.Z. and Y.L. contributed equally. J.Z. and Y.L.: designed the experiments, synthesized and characterized the complex, collated and analyzed the data, and wrote the draft of the manuscript. Z.Z., F.Q., and X.Y. conceived the project and revised the manuscript. All authors have given approval to the final version of the manuscript.

Notes

The authors declare no competing financial interest.

■ ACKNOWLEDGMENTS

This work was supported by the National Natural Science Foundation of China (NNSFC) (no. 82003786); Guangdong Province Basic and Applied Basic Research Fund (nos. 2019A1515110338, 2021A1515220025); and Guangdong Province Medical Research Fund (no. A2023262).

■ REFERENCES

- (1) Siegel, R.; Miller, K.; Jemal, A. Cancer statistics, 2019. *Ca-Cancer J. Clin.* **2019**, *69*, 7–34.
- (2) Liang, S.; Deng, X.; Ma, P. a.; Cheng, Z.; Lin, J. Recent Advances in Nanomaterial-Assisted Combinational Sonodynamic Cancer Therapy. *Adv. Mater.* **2020**, *32*, No. e2003214.
- (3) Chen, H.; Liu, Z.; Jiang, O.; Zhang, J.; Huang, J.; You, X.; Liang, Z.; Tao, W.; Wu, J. Nanocomposite of Au and black phosphorus quantum dots as versatile probes for amphibious SERS spectroscopy, 3D photoacoustic imaging and cancer therapy. *Giant* **2021**, *8*, 100073.
- (4) Grzybowski, A.; Pietrzak, K. From patient to discoverer-Niels Ryberg-Finsen (1860–1904) -the founder of phototherapy in dermatology. *Clin. Dermatol.* **2012**, *30*, 451–455.
- (5) Huang, H.; Banerjee, S.; Qiu, K.; Zhang, P.; Blacque, O.; Malcomson, T.; Paterson, M. J.; Clarkson, G. J.; Staniforth, M.; Stavros, V. G.; Gasser, G.; Chao, H.; Sadler, P. J. Targeted photoredox catalysis in cancer cells. *Nat. Chem.* **2019**, *11*, 1041–1048.
- (6) Dolmans, D. E. J. G. J.; Fukumura, D.; Jain, R. K. Photodynamic therapy for cancer. *Nat. Rev. Cancer* **2003**, *3*, 380–387.
- (7) Monro, S.; Colón, K. L.; Yin, H.; Roque, J.; Konda, P.; Gujar, S.; Thummel, R. P.; Lilge, L.; Cameron, C. G.; McFarland, S. A. Transition Metal Complexes and Photodynamic Therapy from a Tumor-Centered

Approach: Challenges, Opportunities, and Highlights from the Development of TLD1433. *Chem. Rev.* **2019**, *119*, 797–828.

(8) Huang, C.; Liang, C.; Sadhukhan, T.; Banerjee, S.; Fan, Z.; Li, T.; Zhu, Z.; Zhang, P.; Raghavachari, K.; Huang, H. In-vitro and In-vivo Photocatalytic Cancer Therapy with Biocompatible Iridium(III) Photocatalysts. *Angew. Chem., Int. Ed.* **2021**, *60*, 9474–9479.

(9) Zhang, P.; Huang, H.; Banerjee, S.; Clarkson, G. J.; Ge, C.; Imberti, C.; Sadler, P. J. Nucleus-Targeted Organoiridium-Albumin Conjugate for Photodynamic Cancer Therapy. *Angew. Chem., Int. Ed.* **2019**, *58*, 2350–2354.

(10) Fan, W.; Huang, P.; Chen, X. Overcoming the Achilles' heel of photodynamic therapy. *Chem. Soc. Rev.* **2016**, *45*, 6488–6519.

(11) Imberti, C.; Zhang, P.; Huang, H.; Sadler, P. J. New Designs for Phototherapeutic Transition Metal Complexes. *Angew. Chem., Int. Ed.* **2020**, *59*, 61–73.

(12) Novohradsky, V.; Rovira, A.; Hally, C.; Galindo, A.; Viguera, G.; Gandioso, A.; Svitelova, M.; Bresolí-Obach, R.; Kostrhunova, H.; Markova, L.; Kasparkova, J.; Nonell, S.; Ruiz, J.; Brabec, V.; Marchán, V. Towards Novel Photodynamic Anticancer Agents Generating Superoxide Anion Radicals: A Cyclometalated Ir(III) Complex Conjugated to a Far-Red Emitting Coumarin. *Angew. Chem., Int. Ed.* **2019**, *58*, 6311–6315.

(13) Zhao, Q.; Huang, C.; Li, F. Phosphorescent heavy-metal complexes for bioimaging. *Chem. Soc. Rev.* **2011**, *40*, 2508–2524.

(14) Liu, B.; Monro, S.; Lystrom, L.; Cameron, C. G.; Colón, K.; Yin, H.; Kilina, S.; McFarland, S. A.; Sun, W. Photophysical and Photobiological Properties of Dinuclear Iridium(III) Bis-tridentate Complexes. *Inorg. Chem.* **2018**, *57*, 9859–9872.

(15) Jing, Y.; Cao, Q.; Hao, L.; Yang, G.-G.; Hu, W.-L.; Ji, L.-N.; Mao, Z.-W. A self-assessed photosensitizer: inducing and dual-modal phosphorescence imaging of mitochondria oxidative stress. *Chem. Commun.* **2018**, *54*, 271–274.

(16) He, L.; Li, Y.; Tan, C.-P.; Ye, R.-R.; Chen, M.-H.; Cao, J.-J.; Ji, L.-N.; Mao, Z.-W. Cyclometalated iridium(III) complexes as lysosome-targeted photodynamic anticancer and real-time tracking agents. *Chem. Sci.* **2015**, *6*, 5409–5418.

(17) He, L.; Tan, C.-P.; Ye, R.-R.; Zhao, Y.-Z.; Liu, Y.-H.; Zhao, Q.; Ji, L.-N.; Mao, Z.-W. Theranostic Iridium(III) Complexes as One- and Two-Photon Phosphorescent Trackers to Monitor Autophagic Lysosomes. *Angew. Chem., Int. Ed.* **2014**, *53*, 12137–12141.

(18) Peng, K.; Zheng, Y.; Xia, W.; Mao, Z.-W. Organometallic anti-tumor agents: targeting from biomolecules to dynamic bioprocesses. *Chem. Soc. Rev.* **2023**, *52*, 2790–2832.

(19) Zhang, L.; Li, Y.; Che, W.; Zhu, D.; Li, G.; Xie, Z.; Song, N.; Liu, S.; Tang, B. Z.; Liu, X.; Su, Z.; Bryce, M. R. AIE Multinuclear Ir(III) Complexes for Biocompatible Organic Nanoparticles with Highly Enhanced Photodynamic Performance. *Adv. Sci.* **2019**, *6*, 1802050.

(20) Li, L.; Zhang, L.; Tong, X.; Li, Y.; Yang, Z.; Zhu, D.; Su, Z.; Xie, Z. Near-infrared-emitting AIE multinuclear cationic Ir(III) complex-assembled nanoparticles for photodynamic therapy. *Dalton Trans.* **2020**, *49*, 15332–15338.

(21) Liu, S.; Han, J.; Wang, W.; Chang, Y.; Wang, R.; Wang, Z.; Li, G.; Zhu, D.; Bryce, M. R. AIE-active Ir(III) complexes functionalised with a cationic Schiff base ligand: synthesis, photophysical properties and applications in photodynamic therapy. *Dalton Trans.* **2022**, *51*, 16119–16125.

(22) Tong, J.; Yang, X.; Song, X.; Liang, J.; Huang, S.; Mao, H.; Akhtar, M.; Liu, A.; Shan, G. G.; Li, G. AIE-active Ir(III) complexes as type-I dominant photosensitizers for efficient photodynamic therapy. *Dalton Trans.* **2023**, *52*, 1105–1112.

(23) Sun, Q.; Wang, Y.; Fu, Q.; Ouyang, A.; Liu, S.; Wang, Z.; Su, Z.; Song, J.; Zhang, Q.; Zhang, P.; Lu, D. Sulfur-Coordinated Organoiridium(III) Complexes Exert Breast Anticancer Activity via Inhibition of Wnt/ β -Catenin Signaling. *Angew. Chem., Int. Ed.* **2021**, *60*, 4841–4848.

(24) Lv, W.; Zhang, Z.; Zhang, K. Y.; Yang, H.; Liu, S.; Xu, A.; Guo, S.; Zhao, Q.; Huang, W. A Mitochondria-Targeted Photosensitizer Showing Improved Photodynamic Therapy Effects Under Hypoxia. *Angew. Chem., Int. Ed.* **2016**, *55*, 9947–9951.

(25) Tian, X.; Zhu, Y.; Zhang, M.; Luo, L.; Wu, J.; Zhou, H.; Guan, L.; Battaglia, G.; Tian, Y. Localization matters: a nuclear targeting two-photon absorption iridium complex in photodynamic therapy. *Chem. Commun.* **2017**, *53*, 3303–3306.

(26) Gao, Q.; Zhang, C.-Y.; Gao, W.-H.; Wu, Y.; Xie, Y.-B.; Sun, J.-H. Two binuclear lanthanide complexes with 4-quinoline carboxylic acid: crystal structures and luminescent properties. *J. Coord. Chem.* **2009**, *62*, 2689–2697.

(27) Jäger, M.; Eriksson, L.; Bergquist, J.; Johansson, O. Synthesis and characterization of 2,6-di(quinolin-8-yl)pyridines. New ligands for bistridentate Ru-II complexes with microsecond luminescent lifetimes. *J. Org. Chem.* **2007**, *72*, 10227–10230.

(28) Kumar, S.; Hisamatsu, Y.; Tamaki, Y.; Ishitani, O.; Aoki, S. Design and Synthesis of Heteroleptic Cyclometalated Iridium(III) Complexes Containing Quinoline-Type Ligands that Exhibit Dual Phosphorescence. *Inorg. Chem.* **2016**, *55*, 3829–3843.

(29) Fan, Z.; Xie, J.; Sadhukhan, T.; Liang, C.; Huang, C.; Li, W.; Li, T.; Zhang, P.; Banerjee, S.; Raghavachari, K.; Huang, H. Highly Efficient Ir(III)-Coumarin Photo-Redox Catalyst for Synergetic Multi-Mode Cancer Photo-Therapy. *Chem.—Eur. J.* **2022**, *28*, No. e202103346.

(30) Xie, J.; Liang, C.; Luo, S.; Pan, Z.; Lai, Y.; He, J.; Chen, H.; Ren, Q.; Huang, H.; Zhang, Q.; Zhang, P. Water-Soluble Iridic-Porphyrin Complex for Non-invasive Sonodynamic and Sono-oxidation Therapy of Deep Tumors. *ACS Appl. Mater. Interfaces* **2021**, *13*, 27934–27944.

(31) Lamansky, S.; Djurovich, P.; Murphy, D.; Abdel-Razzaq, F.; Lee, H.-E.; Adachi, C.; Burrows, P. E.; Forrest, S. R.; Thompson, M. E. Highly Phosphorescent Bis-Cyclometalated Iridium Complexes: Synthesis, Photophysical Characterization, and Use in Organic Light Emitting Diodes. *J. Am. Chem. Soc.* **2001**, *123*, 4304–4312.

(32) Pei, Y.; Sun, Y.; Huang, M.; Zhang, Z.; Yan, D.; Cui, J.; Zhu, D.; Zeng, Z.; Wang, D.; Tang, B. Ir(III) Complexes with AIE Characteristics for Biological Applications. *Biosensors* **2022**, *12*, 1104.

(33) Zheng, Y.; He, L.; Zhang, D.-Y.; Tan, C.-P.; Ji, L.-N.; Mao, Z.-W. Mixed-ligand iridium(III) complexes as photodynamic anticancer agents. *Dalton Trans.* **2017**, *46*, 11395–11407.

(34) Chen, H.; Ge, C.; Cao, H.; Zhang, X.; Zhang, L.; Jiang, L.; Zhang, P.; Zhang, Q. Isomeric Ir(III) complexes for tracking mitochondrial pH fluctuations and inducing mitochondrial dysfunction during photodynamic therapy. *Dalton Trans.* **2019**, *48*, 17200–17209.